Electronic Supplementary Information (ESI):

The Electrochemical Behaviour of TTF in Li-O_2 Batteries using TEGDME-based Electrolyte

H. Yang, Q. Wang, R. Zhang, B. D. Trimm, and M. S. Whittingham

1. Experimental details

The $LiFePO_4$ and carbon electrodes were prepared by casting slurry onto stainless steel substrate (400 mesh, Ted Pella). The $LiFePO_4$ slurry was prepared by mixing $LiFePO_4$ powder (Primet Inc.), carbon powder (Super C65, Timcal), and polyvinylidene fluoride (PVDF, Aldrich) in an 8:1:1 weight ratio. The carbon slurry was a mixture of Super C65 and PVDF in an 8:2 weight ratio. 1-methyl-2-pyrrolidinone (Aldrich) was used as the mixing solvent. The coated stainless steel substrates were vacuum dried at 75 °C overnight, punched, and transferred to an Ar-filled glovebox for cell assembly. All the $LiFePO_4$ electrodes had active materials loading of around 10 mg (2.85 cm^2), and the carbon electrodes have carbon loading around 2 mg (1.27 cm^2). The loading was designed so that 100 mA/g (cathode carbon loading) was approximately 16 mA/g (0.1 C) for $LiFePO_4$ anodes during charge/discharge cycles. Lithium disks (1.91 cm^2, 0.25 mm thick) were purchased from MTI.

Battery grade 1 M LiTFSI/TEGDME electrolyte was purchased from BASF. TTF and TEGDME were purchased from Aldrich and used as received. TTF was dissolved in the above mentioned 1 M LiTFSI/TEGDME electrolyte or TEGDME solvent to make either 0.05 or 0.1 M TTF-added solution. All solution preparations and cell assemblies were conducted in an Ar-filled glovebox, with moisture and oxygen level always below 1 ppm.

The schematic and photo of the *in-situ* Li-O_2 cell is shown in Fig. S1. The cell was used for the *in-situ* XRD experiments and all the electrochemical tests except the measurement of the redox potential of TTF. Argon or oxygen gas was first dried by a Drierite Gas Purifier and then purged through the *in-situ* Li-O_2 cell for at least 30 minutes before each electrochemical measurement, which was carried out with a MPG2 potentiostat with EC lab software (Bio-Logic Science Instrument). All experiments in this study were carried out at room temperature.

For *in-situ* synchrotron experiments, the cell was mounted on the beamline as shown in Fig. S2. The synchrotron beam comes in the lead slit (2 mm diameter) and out of the wide outlet window. To minimize the effects of synchrotron radiation on the growth and decomposition of Li_2O_2, one pattern was collected for every 15 minutes (shutter closed in between) instead of continuous pattern collection. All the patterns were normalized to the strongest stainless steel peak of the substrate. *Ex-situ* lab x-ray experiments were performed with Scintag XDS2000 θ-θ diffractometer with Cu K_α radiation (λ = 1.5418 Å). The electrodes were rinsed with TEGDME solvent and vacuum dried overnight before XRD patterns were taken.

The redox potential of TTF^+/TTF and TTF^{2+}/TTF^+ were determined by cyclic voltammetry (CV) using a three-electrode glass cell with a platinum wire working electrode and lithium counter and reference electrode. The electrolyte was 0.05 M TTF in 1 M LiTFSI/TEGDME. The scan rate was 20 mv/s. The CV curves of $LiFePO_4$ was collected using the above mentioned *in-situ* Li-O_2 cell with a $LiFePO_4$ working electrode and lithium counter electrode. The electrolyte was 1 M LiTFSI/TEGDME and the scan rate was 0.01 mV/s. Both experiments were carried out inside the argon-filled glovebox.

1. *In-situ* Li-O_2 cell structure and mounting scheme on synchrotron beam line

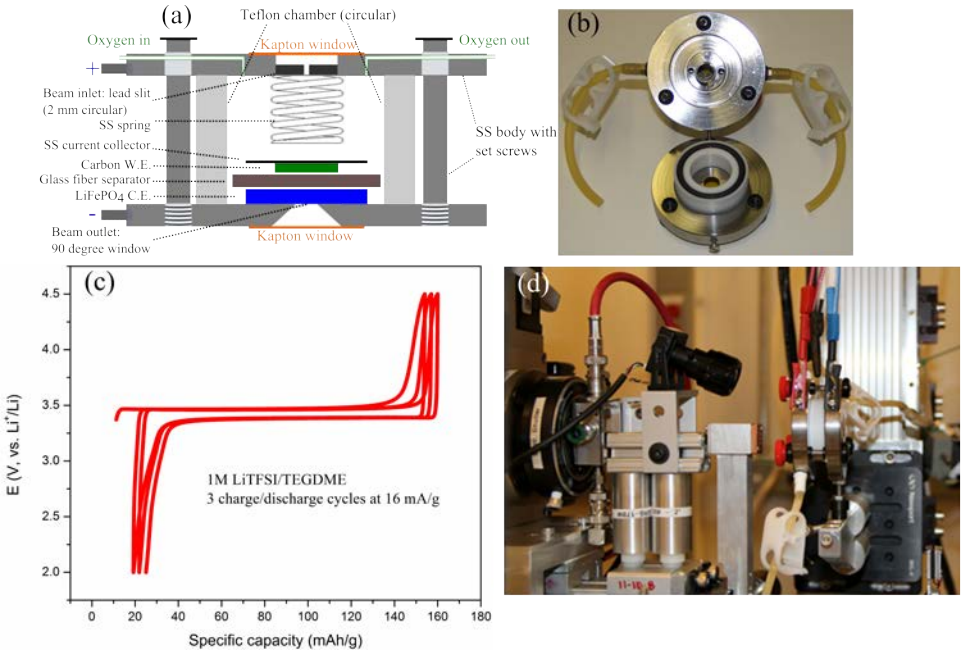

Fig. S1. (a) Schematic and (b) photo of the *in-situ* Li-O_2 cell for synchrotron XRD experiments; (c) charge/discharge tests of the $LiFePO_4$ electrode versus Li with Ar gas purging using the *in-situ* cell, and (d) Cell mounting scheme on 17-BM-B beamline at APS.

Fig. S1 (a) and (b) shows the schematic and photo of the *in-situ* Li-O_2 cell, respectively. The cell is assembled in the following order. First the Teflon ring is placed on the bottom stainless steel (SS) plate. Then anode (lithium or $LiFePO_4$) and separator (glass fiber, GF/B) are placed in this Teflon chamber, followed by adding 200 µL electrolyte. Carbon air cathode and a piece of SS mesh are then placed on top of the stack. The three setscrews guide the top plate to align with the bottom plate. By screwing them down, the central spring presses the cell parts tightly together. At the end of the assembly, the O-rings on both sides of the Teflon ring form tight seal against the corresponding SS plate.

A lead slit with 2 mm center hole was installed on the beam inlet window. The slit was used to guide the beam through the center of the cell so that the diffraction beam went through the wide angle (90 degree) beam outlet window unobstructed. This is done by scanning the beam vertically and horizontally over the lead slit to locate the center point where the diffraction signal is the strongest.

Fig. S1 (c) shows with charge/discharge test curve of a $LiFePO_4$ electrode versus Li anode with Argon purging. A capacity of around 160 mAh/g was obtained for the first cycle. The test was done at 0.1 C for 3 cycles (approximately 60 hours), which is ample time for *in-situ* experiments carried out in this study. The cell can also be used for *in-situ* studies of Li-ion batteries provided that inert gas is constantly purging through the cell.

Fig. S1 (d) shows the photo of the *in-situ* Li-O_2 cell mounted on the beamline 17-BM-B at APS. Similar mounting scheme was adopted at X14A and X18A (NSLS). LaB_6 electrode was

prepared and assembled in the cell in the same manner as carbon electrodes for calibration before conducting *in-situ* experiments.

2. Additional information for *in-situ* synchrotron XRD experiments

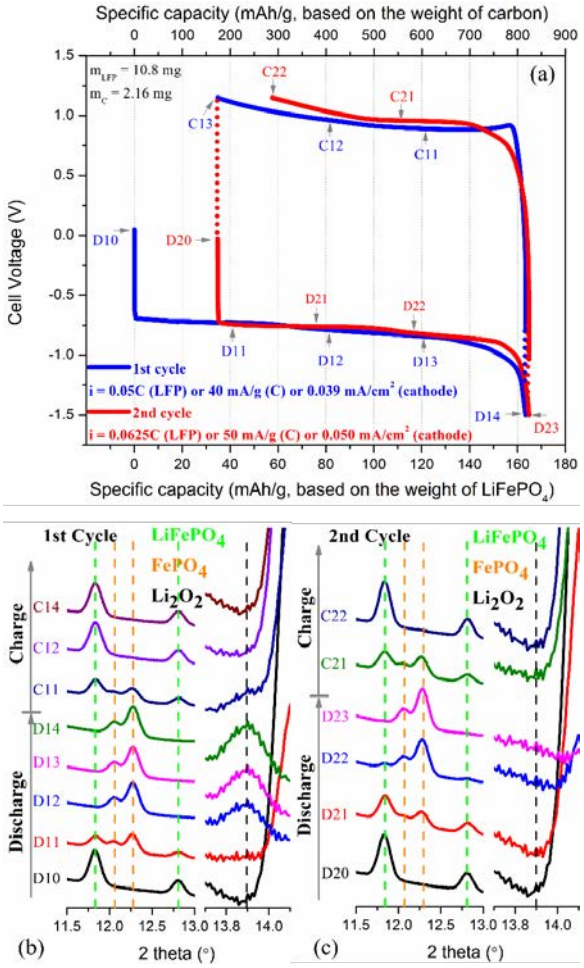

Fig. S2. (a) Discharge/charge profile of a $LiFePO_4$/Carbon-O_2 cell and (b) the *in-situ* diffraction patterns during the first cycle and (c) second cycle (λ = 0.6199 Å).

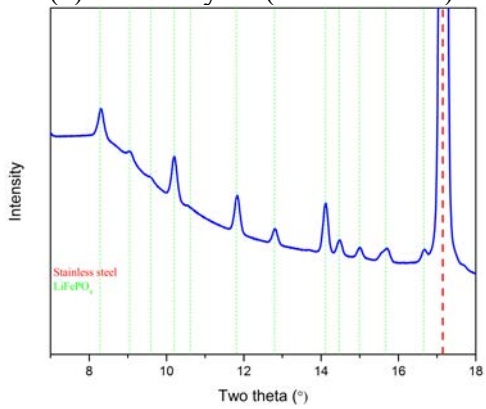

Fig. S3. Synchrotron XRD pattern of the $LiFePO_4$/C cell prior to electrochemical test (λ = 0.6199 Å).

Table S1 Crystal structure information of $LiFePO_4$, $FePO_4$ and Li_2O_2

Phase	Space group	a	b	c	V
$LiFePO_4$ [1]	Pnma	10.34	6.003	4.696	291.7
$FePO_4$ [2]	Pnma	9.810	5.788	4.778	271.3
Li_2O_2 [3]	$P6_3/mmc$	3.169	-	7.714	67.09

The discharge/charge profile of the *in-situ* $LiFePO_4$/carbon-O_2 cell is shown in Fig. S2 (a). The cell was discharged and then charged for two cycles. The discharge corresponds to oxygen reduction reaction (ORR), when $LiFePO_4$ is delithiated on the anode side and Li_2O_2 is generated on the carbon cathode. During charge, oxygen evolution reaction (OER) takes place, which is related to Li_2O_2 decomposition and lithiation of $FePO_4$. The first discharge capacity (163 mAh/g) is close to the capacity obtained from a Li/$LiFePO_4$ cell (Fig. S1), indicating that $LiFePO_4$ anode contributes all the lithium for the ORR reaction. During re-charge, a significant 21.3% capacity loss is observed. Interestingly, all the charge capacity is realized during the second discharge. This shows that the lithium cycles on the $LiFePO_4$/$FePO_4$ anode side for essentially no loss, which contrasts to the huge loss on the cathode side. A slightly lower 17.5% capacity loss is found for the second cycle, which might be related to the passivation film already formed in the first cycle.

Fig. S2 (b) and (c) show the XRD patterns during the first and second cycle in the selected two-theta ranges, respectively. The XRD pattern showing the full two-theta range prior to electrochemical tests are plotted in Fig. S3, together with the diffraction lines expected from the crystal structure information of the phases, $LiFePO_4$, $FePO_4$ and Li_2O_2 (Table S1). Prior to cell discharge, only $LiFePO_4$ phase and peaks from SS substrate can be observed. All *in-situ* patterns are normalized to the strongest SS peak (~ 17 degree at $\lambda = 0.6199$ Å).

As shown in Fig. S2 (b) and (c), the results demonstrate reversible phase transformations of $LiFePO_4$/$FePO_4$ during cell discharge/charge. On the cathode side, Li_2O_2 peak gradually grows towards the end of 1st discharge, and disappears at the end of 1st charge. During the 2nd discharge, no Li_2O_2 peaks can be observed, but the change of the curvature of the background probably indicates that Li_2O_2 becomes amorphous.

These results, though expected, are reported for the first time as *in-situ* monitoring of phase transformations related to lithium shuttling between anode and cathode in Li-O_2 batteries. These evidences are important since coulometric information alone is often found to be very misleading. Employing $LiFePO_4$ anode instead of lithium metal anode, the system is also less prone to side reactions originated from the anode side, for instance, chemical reactions of lithium with moisture and CO_2. The presented $LiFePO_4$/carbon-O_2 cell is thus more suitable for accurate measurement of the cycle efficiency of Li-O_2 batteries.

Despite the fact that some lithium is clearly lost during the cycles, single phase $LiFePO_4$ or $FePO_4$ is observed at the end of charge and discharge in the second cycle, respectively.

Considering the very weak Li_2O_2 peaks, the challenge emerges as the signal-to-noise ratio of the diffraction patterns is not high enough for low intensity peaks. A modified cell that could significantly improve the data quality is under development.

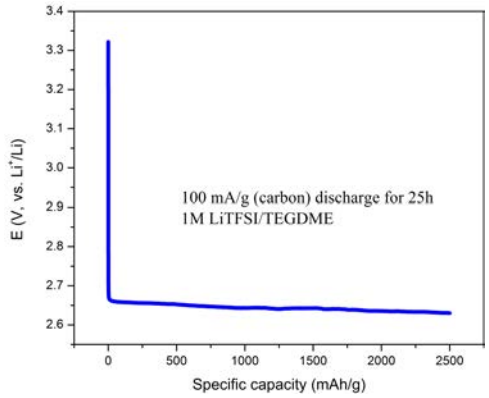

Fig. S4. Discharge a Li/carbon cell in O_2 at 100 mA/g for 25 h.

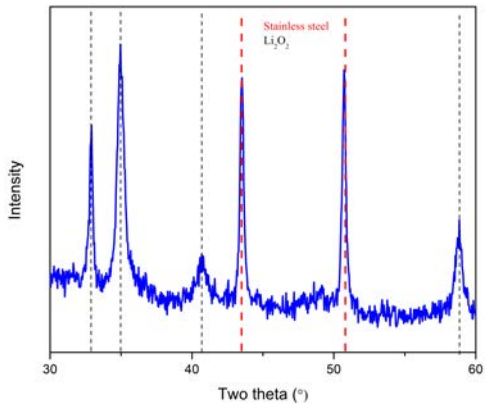

Fig. S5. XRD pattern of a 2500 mAh/g discharged carbon electrode (Cu Kα).

Fig. S4 shows the discharge curve of a Li/carbon cell in O_2 at 100 mA/g for 25 h. Fig. S5 shows the XRD pattern of the discharged carbon electrode. Relatively large amount of Li_2O_2 is deposited on the carbon electrode surface. This discharged electrode is used to assemble the *in-situ* cells as shown in Fig. 2 in the manuscript. It can be seen by comparing Fig. S5 and Fig. 1 (or Fig. S7) that the diffraction signal intensity for Li_2O_2 is much stronger in the pattern obtained by lab XRD.

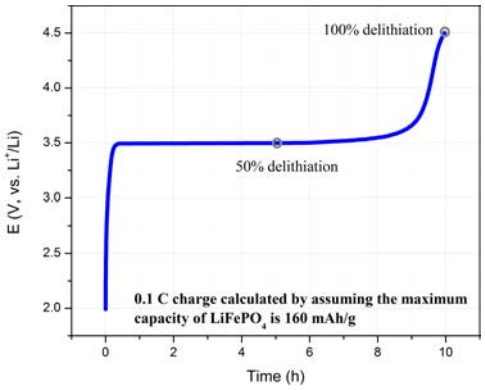

Fig. S6 Electrochemical delithiation curve of $LiFePO_4$ electrode.

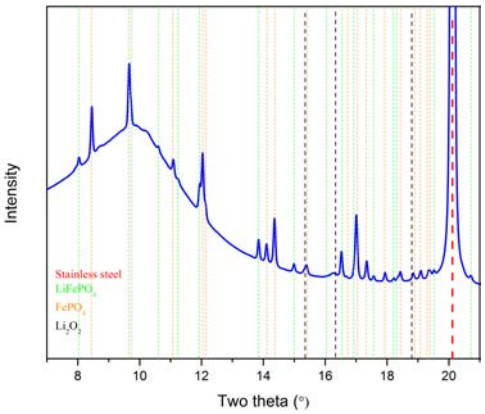

Fig. S7. Synchrotron XRD pattern of the $Li_{0.5}FePO_4$/C-Li_2O_2 cell with TTF-free electrolyte prior to electrochemical test (λ = 0.7270 Å).

Fig. S6 shows the electrochemical delithiation curve of $LiFePO_4$ electrodes. The Li/$LiFePO_4$ half cell was charged at 16 mA/g for 5 h or until fully delithiated (cut-off at 4.5 V). The cell was cycled at the same rate for 3 cycles before the final delithiation process. The as-prepared electrodes were used for the experiments shown in Fig. 2 and Fig. 3 in the manuscript.

Fig. S7 shows the synchrotron XRD pattern for the $Li_{0.5}FePO_4$/C-Li_2O_2 cell with TTF-free electrolyte prior to electrochemical test. The pattern shows $LiFePO_4$, $FePO_4$, Li_2O_2 and SS phases. This is the same cell as shown Fig. 1b.

Fig. S8 shows the synchrotron XRD pattern for the $Li_{0.5}FePO_4$/C-Li_2O_2 cell with 0.1 M TTF-added electrolyte before electrochemical test. It can be seen that $FePO_4$ phase is lithiated during storage with TTF-added electrolyte before the experiments.

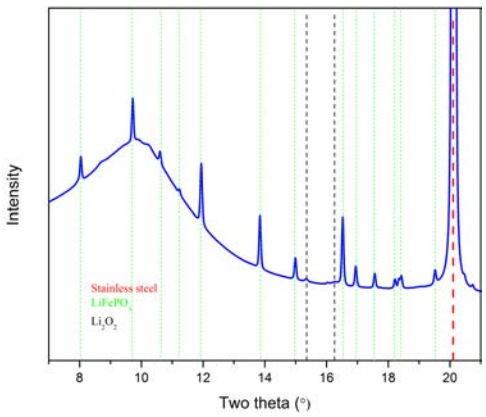

Fig. S8 Synchrotron XRD pattern of the $LiFePO_4$/C-Li_2O_2 cell with 0.1 M TTF-added electrolyte prior to electrochemical test ($\lambda = 0.7270$ Å).

3. Additional information for *ex-situ* studies of the effects of TTF on $FePO_4$ and Li_2O_2

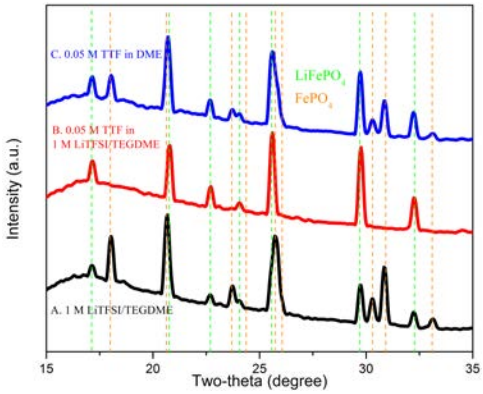

Fig. S9. XRD patterns of the 50% delithiated $LiFePO_4$ electrodes after storage in corresponding electrolyte overnight.

Table S2 ICP results for solutions after overnight storage of a 100% delithiated $LiFePO_4$ electrode and 0.05 M TTF-added 1 M LiTFSI/TEGDME electrolyte.

ppm	Fe	Li	P
I. Diluted with water	0.012	48.154	0.010
II. Diluted with Aqua Regia	0.113	31.484	0.213

Fig. S9 shows the XRD patterns of the 50% delithiated $LiFePO_4$ electrodes after storage overnight in solutions (A) 1M LiTFSI/TEGDME, (B) 0.05 M TTF in (A), and (C) 0.05 M TTF in TEGDME, respectively. It can be seen that the $FePO_4$ phase disappears after soaking the electrode

in solution B, which contains Li^+. The peak intensity of the $LiFePO_4$ phase increases after the lithiation process. After overnight storage of the electrode in solution C, both $LiFePO_4$ and $FePO_4$ phases present as before, however, the peak intensity of the $FePO_4$ phase decreases significantly. The $LiFePO_4$ phase does not seem to be affected significantly.

Table S2 shows the ICP results for solutions after overnight storage of a 100% delithiated $LiFePO_4$ electrode and 0.05 M TTF-added 1 M LiTFSI/TEGDME electrolyte (solution C, Fig. 2). The TTF-added solution is yellow when just mixed. After about 4 hours in contact with delithiated $LiFePO_4$ electrode, the color changes to black. Diluting the black solution with water forms insoluble black suspension. The filtered solution is sample I. Adding a small amount of Aqua Regia dissolves the suspension. The result light black solution is sample II. The ICP results show one magnitude increase in the concentration of Fe and P when Aqua Regia was added. Since Fe and P can only come from the electrode. Therefore, it is suspected that some Fe and P dissolve in or react with the TTF-containing solution. The solution after reacting delithiated $LiFePO_4$ electrode with 0.05 M TTF dissolved in TEGDME solvent was not analyzed (solution B, Fig. 2), but the solution shows similar color change after the reaction (yellow to black).

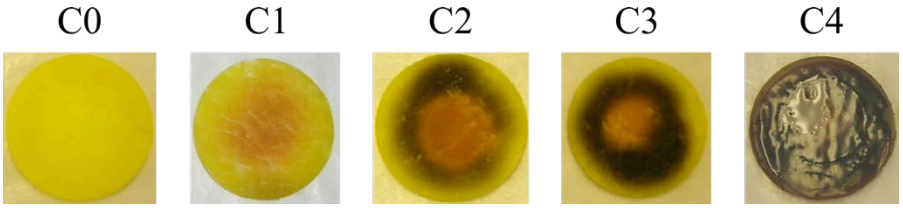

Fig. S10 Color change of the glass fiber separator during charging the Li/carbon cell in O_2 with TTF-added electrolyte.

Fig. S10 shows the color of the separator during cell charging with TTF-added electrolyte. These separators are obtained from the same cell used for Fig. 4c. The color change indicates irreversible reactions, otherwise the yellow color of TTF should be mentained during the cell operation.

References

1. Chen, J.; Vacchio, M. J.; Wang, S.; Chernova, N.; Zavalij, P. Y.; Whittingham, M. S., The hydrothermal synthesis and characterization of olivines and related compounds for electrochemical applications. *Solid State Ionics* **2008,** *178*, 1676-1693.
2. Omenya, F.; Whittingham, M. S., Unpublished data.
3. Chan, M. K. Y., Shirley, E. L., Karan N. K., Balasubramanian M., Ren Y., Greeley J. P., and Fister T. T., Structure of Lithium Peroxide, J. Phys. Chem. Lett. 2011, 2, 2483.